What do trees reveal about the sliding of the lateral moraine of the Belvedere Glacier (western Italian Alps)?

Irene Maria Bollati[1,*], Roberto Sergio Azzoni[1], Anna Tagliaferri[1], Gianluca Tronti[1], Manuela Pelfini[1], Vít Vilímek[2], Lukáš Brodský[3]

[1] University of Milan, Earth Sciences Department , "A. Desio", Italy
[2] Charles University, Faculty of Science, Department of Physical Geography and Geoecology, Czechia
[3] Charles University, Faculty of Science, Department of Applied Geoinformatics and Cartography, Czechia
* Corresponding author: irene.bollati@unimi.it

ABSTRACT

The debris-covered Belvedere Glacier is an iconic place for investigating glacier dynamics and geomorphological processes typical of high mountain environments. Moreover, being located in an area highly suited to tourism, glacial and geomorphological hazards can evolve into risk scenarios. Particular attention has been paid during this research to the surge-type event that occurred at the beginning of the 21st century, and to the recent sliding of a lateral moraine nearby the chairlift station. Tree sampling was performed (19 trees on the lateral moraine; 10 undisturbed trees), and the results were compared with morphometric measurements on orthophotos of different years. Besides sampling trunks, the six available exposed roots (13 samples) from a tree located along the sliding niche were sampled to identify the exposure time. Morphometric measurements of the touristic trail dislocation indicate a sliding rate of 1.87 m/y – 1.98 m/y (2018–2023), while the regression rate of the sliding niche is 1.70 m/y (2021–2023). The age of trees along the trench is variable (14–49 years), as is the signal of compression wood, enhancing differentially the passage of the surge wave and the subsequent glacier downwasting. The beginning of root exposure occurred between 2017 and 2019, before the effective evidence of large fractures in the ground. Moreover, the roots show traumatic resin ducts in the period between 2020 and 2022, confirming the tree disturbance. In conclusion, the investigated events are recorded differentially in the sampled trees, especially in roots, anticipating the actual commencement of ground failure. A multidisciplinary approach, including remote sensing, field survey, and dendrogeomorphological analysis is essential to define the dynamics of complex systems.

KEYWORDS

dendrogeomorphology; paraglacial dynamics; surge-type event; moraine sliding; Belvedere Glacier

Received: 3 April 2024
Accepted: 2 September 2024
Published online: 14 October 2024

Bollati, I. M., Azzoni, R. S., Tagliaferri, A., Tronti, G., Pelfini, M., Vilímek, V., Brodský, L. (2024): What do trees reveal about the sliding of the lateral moraine of the Belvedere Glacier (western Italian Alps)?. AUC Geographica 59(2), 255–271
https://doi.org/10.14712/23361980.2024.14

1. Introduction

The debris-covered Belvedere Glacier, located on the eastern side of Monte Rosa (Western Italian Alps) (Fig. 1a), is an iconic area in the European Alps. Together with the Miage Glacier, another peculiar debris-covered glacier located in the Mont Blanc Massif (Italian side) (Bollati et al. 2015), it represents one of the most deeply studied glacial areas in the Italian Alps. The glacier has an extensive debris coverage, which is not so common in the European Alps, and a very peculiar morphology, similar to the Miage Glacier, with the glacial snout divided into two lobes. It presents a complex response to climate change, marked by altered surface ablation rates and spatial patterns of mass loss, as generally observed in debris-covered glaciers in other mountain ranges (e.g., Benn et al. 2012). Since debris coverage can reduce the ablation rate when it exceeds a critical thickness (e.g., Nakawo et al. 1999; Fyffe et al. 2014; Mehta et al. 2023), the Belvedere Glacier maintains its front at relatively low elevations (approximately 1800–1900 m a.s.l.), below the tree line. On the contrary, Belvedere tributary glaciers, not covered by debris, are undergoing a fast retreat in line with the overall trend in the European (Paul et al. 2020) and Italian Alps (Smiraglia and Diolaiuti 2015). Even if this trend may vary depending on the glacier types, since valley glaciers are found to be less sensitive to air temperature and precipitation (Serandrei-Barbero et al. 2022), this trend is leading to the separation of Belvedere from the tributary glaciers.

Despite the snout of the Belvedere Glacier remaining at relatively low elevations, constant in-situ monitoring (Mortara et al. 2023) and recent photogrammetric studies provide evidence of downwasting, gradual glacier retreat, and morphological modifications (Ioli et al. 2023; Brodský et al. 2024, in this issue).

The scientific interest derives from the different kind of processes (glacial, gravity-, and water-related) potentially generating hazards in the area (Mortara et al. 2017). For instance, the Glacier Lake Outburst Floods (GLOFs) from Lake Locce (1970, 1978, and the most recent one in 1979; Mortara and Tamburini 2009; Kääb et al. 2004) posed serious issues, since they affected localities in the municipality of Macugnaga (i.e., the destruction of the lower chairlift station and the sudden increase of solid and liquid discharges along the Anza River). As a response to these events, several investigations and interventions to mitigate the risk scenarios were planned in the area (VAW 1983, 1985). Considering the 21st century in more detail, the most relevant geomorphological processes related to the Belvedere Glacier and its surrounding areas, interfering in some way with the glacier dynamic and also generating hazards downvalley, were: a surge-type event, characterized by glacier changes between 1999 and 2003, and reaching the acme between 2000–2002 (Mazza 2003; Kääb et al. 2004); the formation and evolution of an ephemeral lake (Lake Effimero; Fig. 1a) whose GLOF is a potential threat to Macugnaga village; significant rock falls and avalanches (2005, 2007) sometimes also accompanied by ice (Fig. 1a); the Castelfranco debris flow that recently hit the glacier area in August 2023 (Fig. 1a); and, finally, the continuous sliding of lateral moraines (Fig. 1a).

Most of these processes may be classified as paraglacial-type processes i.e., according to Church & Ryder (1972) "… non-glacial processes that are directly conditioned by glaciation". They refer both to "proglacial processes, and to those occurring around and within the margins of a former glacier that are the direct result of the former presence of ice". Ballantyne (2002) classified a series of paraglacial-type processes, among which there is the debuttressing of lateral rocky and debris slopes along glacial valleys, favoring rock falls and avalanches, and landsliding in general. The latter is a process continuously affecting the Belvedere area (Mortara et al. 2023), especially since the end of the Little Ice Age (14th century CE – 1850–1860 CE; Ivy-Ochs et al. 2009), but it became more significant after the sudden exhaustion of the 2000–2002 surge-type event, as the support offered by the huge ice volume disappeared quite rapidly.

Since the snout of the Belvedere Glacier is located below the tree line, the moraines bordering the central-lower part of the glacier, including the one undergoing sliding, are colonized by broadleaves and coniferous trees of different species. Among them, larches (*Larix decidua* Mill.) are pioneer species also colonizing unstable surfaces and constituting an early step in the renewal of the ecological series.

In the literature, dendrochronological analyses, based on tree rings, have been performed on larch and coniferous species in high altitude environments to detect climatic signals (e.g., Leonelli et al. 2016), or to reconstruct geomorphological disturbances in different geomorphological contexts, such as landslides (e.g., Fantucci 1997; Guida et al. 2008; Tichavský et al. 2019), debris flows (e.g., Garavaglia et al. 2009; Bollati et al. 2018), or snow avalanches (Garavaglia and Pelfini 2011; Bollati et al. 2018; Favillier et al. 2023), as well as in glacial contexts for detecting glacier fluctuations, mass balance, surface instability (e.g., Pelfini 1999; Richter et al. 2004; Leonelli et al 2008; Leonelli and Pelfini 2013), and also proglacial stream activity (e.g., Pelfini et al. 2007; Garavagliaet al. 2010).

Several morphological (micro and macro) indicators in tree rings (i.e., growth anomalies, compression wood, eccentricity index, traumatic resin ducts; Pelfini et al. 2007; Stoffel and Bollschweiler 2007) are used to reconstruct such dynamics. Their reliability may vary accordingly; for instance, to the type of process and to morphological features of the sites (de Bouchard d'Aubeterre et al. 2019). Moreover, when

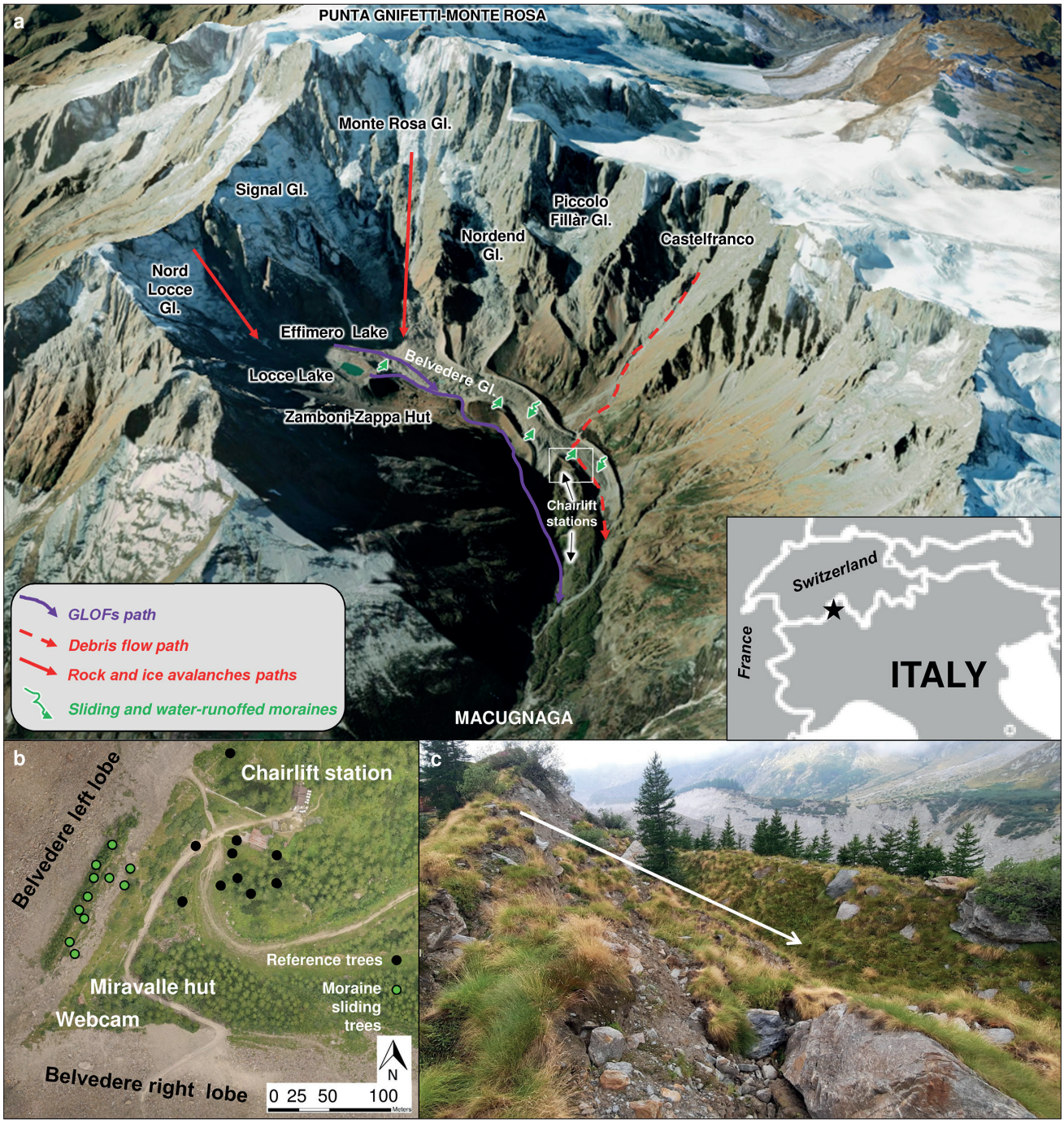

Fig. 1 The head of the Belvedere Glacier hydrographic basin on a Google Earth 3D image with the white square indicating the study area and referring to Fig. 1b, c, and the path of the most significant geomorphic processes affecting the area (a); the tree sampling distribution on the orthophotos, created in 2023 using a drone flight (b), and an image of a trench related to moraine sliding (c).

tree roots are exposed along erosion surface, they may also be used to date the sediment removal and to calculate average erosion rates (e.g., Stoffel et al. 2013; Bollati et al. 2016).

Concerning dendroglaciological analyses in the Italian Alps in more detail, and firstly considering the case of a debris-free glacier, Pelfini (1999) detailed the advance of the Grande di Verra Glacier (Aosta Valley, Italian Alps) as far as the Little Ice Age (14th century CE – 1850–1860 CE; Ivy-Ochs et al. 2009), as well as the retreat phases, through the analysis of tree ring width anomalies. On the other hand, the glacial dynamic of a debris-covered glacier is even more particular. The position of the debris-covered glacier snout remains quite constant despite the mass transferring through kinematic waves crossing the glacier as far as the snout, the crevasses or the ice cliffs, where the mass wasting is greatest. In the case of the Miage glacier (Aosta Valley, Italian Alps), for instance, there is a proper forest growing on the glacier debris coverage, and the analyses of tree rings enabled the passage of a kinematic wave in 1980s to be detected,

differentially on its two lobes (i.e., 5-years delay; Pelfini et al. 2007; 2012).

In both these cases, the data extracted from the tree cores provided information at an annual resolution, which may be further discussed in comparison with data from remote sensing analyses (e.g., velocity of the glacier flow, surface topographic change), based on aerial images and digital elevation models with different space and time resolution (e.g., Azzoni et al. 2023).

In this work, the aim was to analyze in detail the response of the lateral moraine of the Belvedere Glacier nearby the chairlift station to the pressure it underwent during the surge-type event, to the ongoing relaxation due to glacier downwasting (e.g., paraglacial debuttressing, sensu Ballantyne 2002), and to water runoff affecting the moraine's inner flank. To achieve this, the traditional tree ring indicators and dendrogeomorphological investigations were used and compared with field observations, and morphometric data from remote sensing analyses.

2. Study area

The Belvedere Glacier is one of the most famous debris-covered glaciers in the European Alps, renowned for its debris coverage and its location just below the base of the east side of Monte Rosa, the highest European alpine wall. It is located at the head of the Anzasca Valley (Western Italian Alps), on the border with Switzerland (Fig. 1). The debris coverage is fed by ice and snow avalanches, and rock falls, frequently originating from the eastern face of Monte Rosa (Giordan et al. 2022). The Belvedere Glacier is hence featured by an elevated sediment coverage (i.e., Monterin 1923, Mazza 1998; Haeberli et al. 2002). The forest surrounding, but also connected with the glacier environment, is formed by European larch (*Larix decidua* Mill.), Norway spruce (*Picea abies* Karst), and other alpine species such as birch (*Betula pendula*) and green alder (*Alnus alnobetula*) in wetter areas. Above the climatic tree line, located at 2215 m a.s.l. (Tampucci et al. 2017), open environments prevail, characterized by extensive rocky surfaces, screes, moraines, and remnants of acidic substrates from glaciers where alpine scrub or scrubland comprise primarily of green alder, and rhododendron (*Rhododendron ferrugineum*). The vegetation growing on the Belvedere Glacier is distinct, as exists in a colder environment compared to the surroundings. It hosts unique assemblages of cold-adapted plant species, which remain unaffected by glaciological variations within debris-covered glaciers (Tampucci et al. 2017). This characteristic makes it a potential warm-stage refuge for cold-adapted species (Cacciani ga et al. 2011). Compared to similar environments (i.e., the Miage Glacier, Pelfini et al. 2007; 2012), the vegetation and trees on its surface have considerably younger ages, up to 5–6 years old.

Vegetation has to cohabit within a highly dynamic environment. Indeed, despite the seemingly stable position of its front, composed of two distinct lobes (left and right in this work; see Fig. 1), the Belvedere Glacier is undergoing dramatic changes, particularly in terms of glacier thickness (e.g., Ioli et al. 2021; De Gaetani et al. 2021; Ioli et al. 2023; Mortara et al. 2023).

Moreover, after the separation from of the Nordend Glacier and the Nord Locce Glacier, the Belvedere Glacier is now solely fed by the very steep Monte Rosa Glacier. However, this connection may also be compromised in the near future due to global warming if glacier retreat continues.

Several authors have estimated the losses and gains of Belvedere ice volumes since the middle of the 20th century using topographic maps, digital elevation models, and punctual measurements through ice stakes. Tab. 1 provides a summary of the main results in the literature of the ice volume variations, and the ice flow velocities are also included.

An important event that occurred in the study area, attracting the attention of several scientists, was the surge-type event (i.e., kinematic wave), that, considering all the possible evidences, was observed in the 1999–2003 timeframe (Kääb et al. 2004). Details are provided in section 2.1. De Gaetani et al. (2021) calculated an acceleration of ice thickness (and volume) reduction during the period between 2001 and 2009, during and after the end of this surge-type event based on five surveys conducted on the glacier between 1977 and 2019. In particular, during the 2009–2019 the volume loss propagated towards the glacier snout, which began in 2001 from higher elevations. In total, a loss of 54 million m^3 of ice was calculated by the authors during the 1977–2019 time interval.

When, then, the moraine under investigation began to collapse (2015–2020), Ioli et al. (2021) measured an ice loss rate of between 2 and 3.5 million m^3/y, lower than the values calculated immediately after the surge, but detecting an active downwasting nevertheless.

Mortara et al. (2023) calculated the punctual ablation between 2010 and 2023 testifying to a variable annual surface lowering of between 270 and 430 cm with maximum values in 2015. They also recorded a decrease in velocity during the 1987–2023 time interval, interpreted as the slowing down of the ice mass transfer from the accumulation to ablation zone favoring the glacier snout retreat. Again, in terms of velocity, Ioli et al. (2021) found variable values in the different areas of the glacier. In normal periods, the data in the literature report a velocity of between 2 and 43 m/y, while during the surge-type event it reached values of 100–200 m/y (Tab. 1; Kääb et al. 2005; Ioli et al. 2021).

Tab. 1 Summary of the main measurements of ice volume and surface velocity variations present in literature.

Time interval	Author	Volume (million m3)	Rate (million m3/y)	Note
1957–1991	Diolaiuti et al. (2003)	+22.7	0.69	
1983–1985	Roethlisberger et al. (1985)		+1.50	
1977–1991	De Gaetani et al. (2021)	+10.06	+0.72	
1991–2001		+10.61	+1.06	Before surge
1977–2001		*+20.66*	*+0.72*	*Before surge*
2001–2009		−47.78	−5.97	During surge and after
2009–2019		−27.16	−2.72	Before the moraine collapse
1977–2019		*−54.28*		
2015–2020	Ioli et al. (2021)		2.0–3.5	Before and during the moraine collapse
Time interval	**Author**	**Surface velocity (m/y)**		**Note**
1995–1999	Kääb et al. (2005)	32–43		
2001		100–200		
2015–2020	Ioli et al. (2021)	17–22		Central portion
2015–2020		2–7		Accumulation zone and glacier snout

After the surge-type event a total retreat of the glacier snout of 300-m was measured by Mortara et al. (2023). The glacier snout morphological modifications were also measured by Ioli et al. (2023) through an innovative photogrammetric technique, indicating an average glacier retreat rate of 2.7 m in one month (July–August 2022), and an ice volume loss of approximately 14×10^3 m^3.

In this historical framework of the Belvedere Glacier, two events are considered for the present study, both affecting the area below the tree line, in a period overlapping with the tree chronologies: the surge-type event between 2000 and 2002, and the moraine collapse at the chairlift station and near the Miravalle hut and in subsequent years, highlighted by ground failures in 2019. These events are described in detail in the following sections.

2.1 The surge-type event

The surge-type event with first evidences in 1999, reached the acme during the summer of the year 2000 till the late spring of 2002, exhausting in 2003 (Mazza 2003; Kääb et al. 2004). The deep morphological changes affecting the glacier made this event quite unique in the European Alps. The three main features of this event, described by Mortara et al. (2023), are: i) the increase in superficial velocity, ii) the intense crevassing of the glacier tongue, and iii) the local increase in the volume and thickness (up to 20 m; Kääb et al. 2004). This allowed the ice to overwhelm the Little Ice Age moraines, especially on the right side, near the Zamboni-Zappa hut, and filling the breach in the moraine generated during the previous Lake Locce GLOFs (Mortara and Tamburini 2009). During the surge-type event, indeed, a glacial mass transformation and transfer occurred: the glacier terminus moved downvalley for 40 m. The measured velocity was 100–200 m/y (Kääb et al. 2005) compared to the normal 20–30 m/y (Mortara and Tamburini 2009). According to Haeberli et al. (2002), in the summer of 2000, the Monte Rosa glacier flowing into the Belvedere accelerated its flow, as testified by several crevasses, and induced compression and deformation on the Belvedere ice mass. Evident new moraines are now the past witnesses of this surge-type event, especially along the right moraine, and the right side of the left lobe, downvalley in regard to the lobe separation. Haeberli et al. (2002) underlined how this process may have triggered potential hazards for the infrastructure in the area, and also downvalley, if pressurized water came out, for instance from an ephemeral lake formed during the surge-type event. For this reason, it was observed and monitored in detail to set specific rescue strategies with the local authorities (VAW 1983, 1985).

After the event, the dramatic ice downwasting induced a generalized instability along the lateral moraines, leading to their subsequent degradation, and collapse and hazards related to the surge-type event have continued some years after the end of the event.

2.2 Sliding of the lateral moraine at the Miravalle hut

After the exhaustion of the surge-type event, the Little Ice Age degradation of the lateral moraines, for the paraglacial debuttressing and water runoff on the inner flank of the moraine no longer covered by ice, induced sliding and genesis of pseudo-badlands morphology (Curry and Ballantyne 1999; Klimeš et al. 2016; Bollati et al. 2017).

The greater effects of the decrease in ice thickness after the surge-type event were recorded along the up-valley portion of the right lateral moraine (Mortara et al. 2023). Along the other moraines, the instability

is also still ongoing, which is matter of concern due to the tourist and alpinist trails along the moraines (Tamburini et al. 2019; Mortara et al. 2023). For instance, in the summer of 2023, the local authorities attempted to reconstruct the trail to Zamboni-Zappa hut through intense excavation on the moraine and regularization of the glacier surface of the right glacier lobe. The aim was to create a larger path also usable by excavators. However, this track underwent rapid degradation (within two months), especially on the unstable portion descending the inner flank of the left moraine of the right lobe and crossing the glacier.

Nearby the chairlift station, used by skiers in winter and mountaineers in summer, the right moraine of the left lobe, the object of interest for this study (see Fig. 1), has being affected by large fractures since 2019. This process is decreasing the trail stability along the moraine ridge, which is not walkable anymore and has been moved to the external flank of the moraine. In addition, the Meteo Live VCO webcam, located at the lobe divide, undergoing destabilization, eventually fell in May 2024, as a consequence of heavy rains probably combined with snow melting (see Fig. 2). During the second half of July 2019, when the fracture was detected, Tamburini et al. (2019) calculated a glacier surface lowering of approximately 46 cm (4.6 cm/day). During the period between 2015 and 2020, the rate of ice volume loss was estimated to be 2.0–3.5 million m^3/year (Ioli et al. 2021). The investigated moraine is located in sector S3, one of the three sectors identified by Ioli et al. (2023). This low relief sector is particularly stressed: the glacier splits in two different lobes, the authors detect a velocity of approximately 2–7 m/y, and the crevassed area up valley from the glacier division features a very high variability of surface velocity.

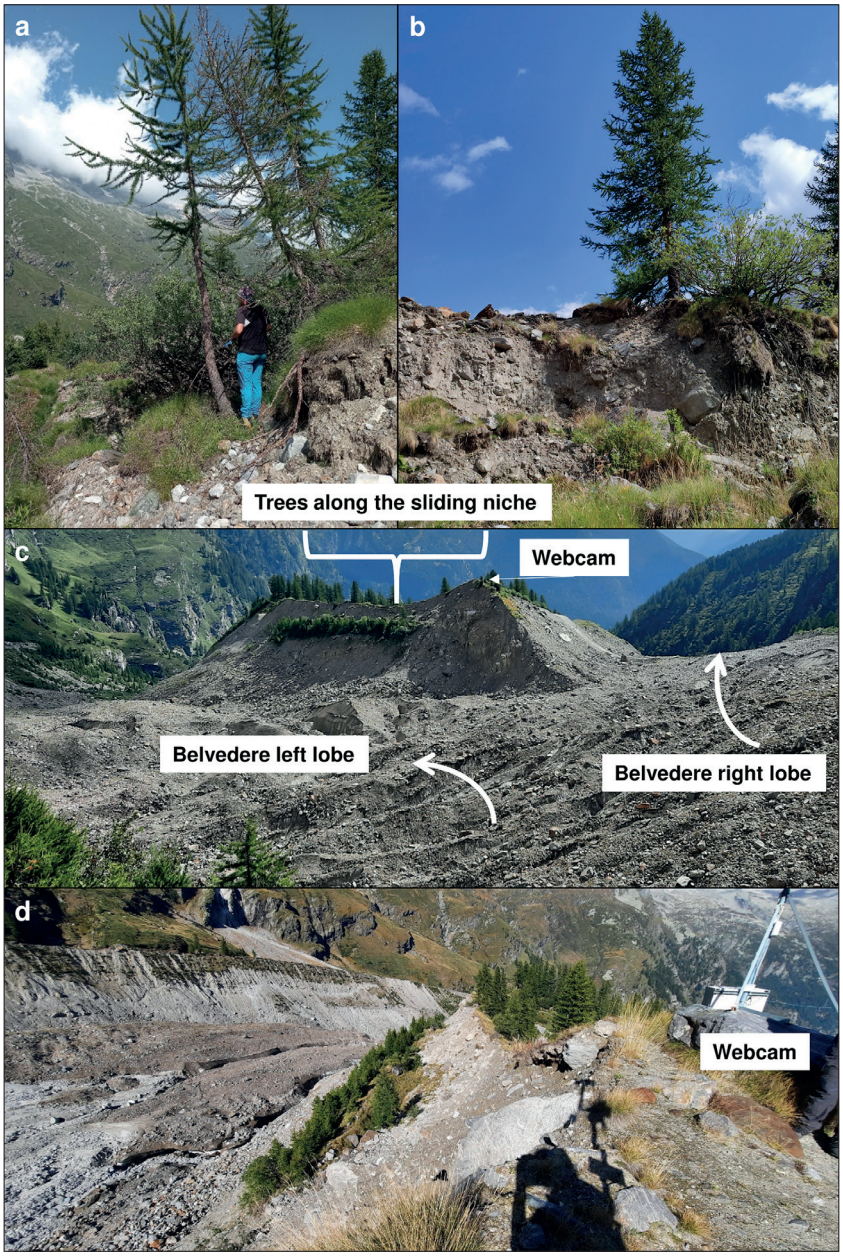

Fig. 2 Examples of trees in the unstable portion of the right moraine of the left lobe of the Belvedere Glacier (a), and a view of the sliding moraine from the opposite side of the glacier, as well as from the Meteo Live VCO webcam, lost in May 2024.

As the collapsing moraine is at a lower elevation than the tree line, it is colonized by coniferous and broadleaves species, as described in detail previously. Fig. 2a and 2b provide examples of trees along the sliding niche, which are investigated in this study as potential data loggers for tracking sliding movements. The aim is to detect the reliability of trees in understanding, with annual resolution, when the movement effectively began and whether it corresponded to the opening of the fracture in 2019. Fig. 2 shows the sliding moraine from the opposite side of the glacier (c) and the extensional trench visible from the Meteo Live VCO webcam, unfortunately now lost (d). The trench is also well visible in Figure 1 (c), and on the orthophoto from the Unmanned Aerial Vehicle (UAV) flights performed in August 2023 (Fig. 1b).

3. Material and methods

3.1 Geomorphological mapping and morphometric measurements

Mapping of geomorphological features was performed in detail nearby the sliding moraine, to survey the main geomorphic signs of the sliding. The mapping was included in the ongoing broader geomorphological mapping activity covering the entire Belvedere Glacier area. The landforms were classified according to their genetic processes (e.g., gravity, glacial) and particular attention was paid to morphodynamic conditions because of their potential relation to hazard scenarios (Bollati et al. 2024). In addition, landforms deriving from human activity were also mapped. The manmade elements, such as the remodeled surfaces, the chairlift infrastructure, and the old tourist trail along the moraine ridge, leaving evident signs on the landscape, were also considered.

Morphometric measurements were performed to quantify the sliding and the retreat of the niche (Fig. 3). The tourist trail not involved in the sliding (T1), and the one that ran along the moraine ridge, and that was lost (T2), were useful for estimating the surface displacement. Two different features were measured to quantitatively assess the displacement using the orthophotos from 2018 (the last year before the appearance of the field evidence, AGEA orthophoto, average resolution 0.30 m) 2021 (AGEA orthophoto, average resolution 0.30 m), and 2023 (year of the drone survey in the area, 0.05 m):

– *Sliding of the moraine ridge* using two features: i) tourist trail displacement calculated as the distance between the location of trail T2a on the 2018 orthophoto, T2b on the 2021 orthophoto, and T2c on the 2023 orthophoto (Fig. 3); ii) difference between the distance between trail T1, which was not affected by instability (Fig. 3), and the tree canopy on the moraine ridge before (2018 orthophoto) and during the sliding (2021 and 2023 orthophotos). The linearity of elements used for measurement in the i-method provided more accurate data with an error related to the resolution of the image (variable between 0.05–0.3 m, i.e., orthophoto resolution). In the second case (ii-method), the measurements were based on tree canopies growing on the moraine ridge, and their detection on the orthophotos from 2018 and 2021 was quite challenging. A greater specimen or particular clusters of trees were considered, since they were more easily detectable on the images. Nevertheless, these measurements are considered not in an absolute sense but as a confirmation of the i-measurements.

– *Regression of the sliding niche*: calculated as the distance between the position of the sliding niche

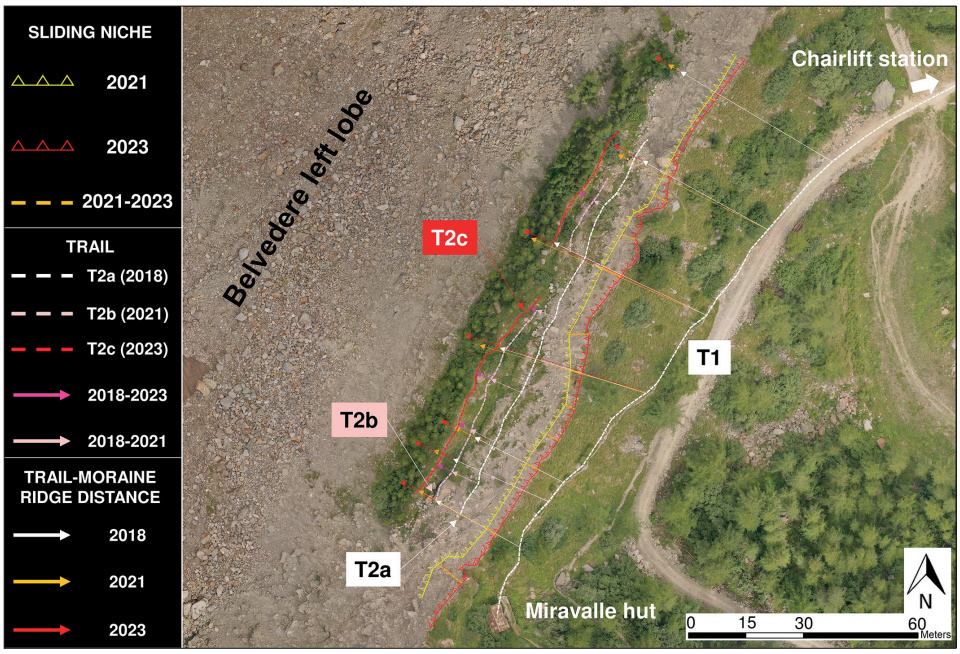

Fig. 3 Displacement measurements along the sliding moraine. The trail and the moraine ridge displacement are indicated (different colored arrows), as well as the regression of the sliding niche (orange dashed line) considering the orthophoto from 2018 2021 by AGEA; and 2023 resulting from the UAV flight performed in August 2023. The latter is also the background of the image.

on the 2021 orthophoto and the 2023 orthophoto (Fig. 3).

In addition to the displacement, average rates of sliding and retreat were calculated for the different time intervals. Two rates were calculated: one considering the year of the last orthophoto available before the sliding (2018), and another considering the year of ground fracture observation (2019) reported in the literature (Mortara et al. 2023).

3.2 Dendrogeomorphological analyses

Field sampling was performed in 2021 and 2022 (Fig. 4b, c) in order to collect samples from trees and exposed roots mostly stressed by the processes of sliding. Fig. 1 (b) shows the location of the sampled trees for dendrogeomorphological analyses. It should be noted that some tree positions taken with the GPS represent a cluster of trees due to GPS error (approximately 3 m).

Samples from tree trunks were taken using a Pressler increment borer. The cores extracted from the trunks were collected in most cases at the standard height of the trunk of 1.30 m (chest height), but because the sample locations were quite unstable, and in some cases very hard to access, the samples were sometimes taken nearby the base of the trunk, also to obtain the longest chronology as possible. Nevertheless, the aim of the analysis was not to date the germination of the trees or the surface stabilization and relative colonization by trees; hence, the minimum age of trees was only considered, and no corrections were made based on the sampling height. In total 19 trees growing along the lateral moraine (48 cores) in the newly formed trench, and 10 trees (20 cores) in an undisturbed area were sampled for a total of 68 cores analyzed. The tree chronologies and ring features of reference trees were compared with those of disturbed trees to detect the possible differences in relation to active geomorphic processes.

Moreover, disks were cut from the available six exposed roots (13 samples) from one of the trees (No. 6) located along the sliding niche, to determine when the effective exposure began. The changes in the tree root micromorphology, from the production of root-type wood to trunk-type wood, were used to detect the exposure year. Root exposure is also useful for estimating the average erosion rate over the exposure period. This may be calculated as the ratio between the thickness of the removed sediment and the time interval since the exposure (e.g., Hupp and Carey 1991 Pelfini and Santilli 2006; Stoffel et al. 2013; Bollati et al. 2016). A significant uncertainty may be introduced during this calculation (Bodoque et al. 2015), especially in complex contexts of an exposure of this type. Hence, in this specific case, we decided not to measure the erosion rate through the removed sediment thickness, but to focus on the different years of exposure obtained from roots, comparing them with the calculated values through morphometric techniques using orthophotos (see Section 3.1).

After preparing the tree cores and root disks, the ring widths were measured (accuracy of 0.01 mm) using the LINTAB and TSAP systems (Rinn 1996) and image analysis using WinDENDRO software (Régent Instruments Inc. 2001). The cross dating of the dendrochronological series was performed visually with TSAP, considering the Gleichläufigkeit (GLK), the Cross Date Index (CDI) and the Generalized Level of Significance (GLS) coefficients, to establish the date of each individual annual ring. GLK (Eckstein and Bauch 1969) compares the similarity between two growth curves based on the concordance and discordance of curves' tendency, while GSL, depicts the significance of the GLK value, and CDI represents the synthesis of the similarity tests (GLK, GSL) conducted between the curves (Schmidt 1987). The detrending of the tree growth curves for the autocorrelation removal was performed with the Arstan software (Cook 1985), and after this phase, the cross-dating was checked again. The growth disturbances in the tree cores were finally analyzed (i.e., compression wood, growth anomalies, traumatic resin ducts). Since consideration of the percentage of trees affected by disturbance is influenced by the number of trees present in a specific year, according to the age of the trees, the time frame considered for the analysis began in 1997, i.e., when at least 50% of the trees were present.

The following disturbance indicators were selected for the analysis:

i) *Growth anomaly index* (e.g., Pelfini et al. 2007; Bollati et al. 2016): it is useful for analyzing abrupt growth changes (i.e., release and suppression) and it is based on the yearly percentage growth variation with respect to the mean of the four previous years. The growth anomaly index was calculated after detrending and autocorrelation removal. For the plotting, specific threshold values for growth suppression in trees (Negative Anomaly Index – NAI), potentially related to suffering, were then considered, with thresholds of 40% and 70% for negative anomalies (as adopted by Pelfini et al. 2007), while specific thresholds for positive growth anomalies were not distinguished. The NAIs were calculated for both disturbed and reference trees to determine which NAIs may be related to the local conditions of geomorphic disturbance or to a more general disturbance according to the considered species. In NAI investigation, it is important to consider in particular the climate effect. The growth of European larix above 1400 m a.s.l. is driven positively by high summer temperatures, warm autumn temperatures, and abundant July precipitation, also considering favorable microclimatic conditions (Saulnier et al. 2019). If the anomalies are common between trees in disturbed and reference clusters, the anomaly may be related to unfavorable climate conditions

or other regional impacts (e.g., insect attack; Vejpustková and Jaroslav 2006). The NAI, especially the positive values, were also considered for raw growth curves of roots since after exposure a growth release is usually found (Pelfini and Santilli 2006; Bollati et al. 2016). For the growth anomaly calculation, the analysis extends from 1997 to 2021, since 2022 was not in all the cases a complete ring.

ii) *Compression wood (CW)* (Timell 1986): it is a particular, denser kind of wood, being a response to mechanical stress. The space–time distribution of CW among the trees along the trench and sliding moraine ridge, and sliding niche, was assessed through the occurrence on the tree cores. Also, a compression-type wood may appear in roots after exposure (Pelfini and Santilli 2006). For the compression wood analysis, as opposed to the NAI analysis, which ended in 2021, the year 2022 was also considered, even if not completed, as the CW could be visually detected and it may indicate the continuation of the disturbance.

iii) *Traumatic resin ducts (TRDs)* (e.g., Bollschweiler et al. 2008): these appear as a continuous row of resin ducts in earlywood or latewood, and they are considered indicators of the tree undergoing trauma. TRDs, often associated to scars, may show when the plant needs a greater support of resin, during very intense stress, and they may also appear in roots (Cruickshank et al. 2006). The disturbance may be caused by geomorphic events (e.g., debris flows or snow avalanches, Bollschweiler et al. 2008) but also by fires and insect attacks (Cruickshank et al. 2006).

The investigation of tree ring anomalies focused on finding a possible relation to the main glaciological events (surge-type event and moraine sliding) that occurred in the timeframe when the moraine tree and root chronologies overlap.

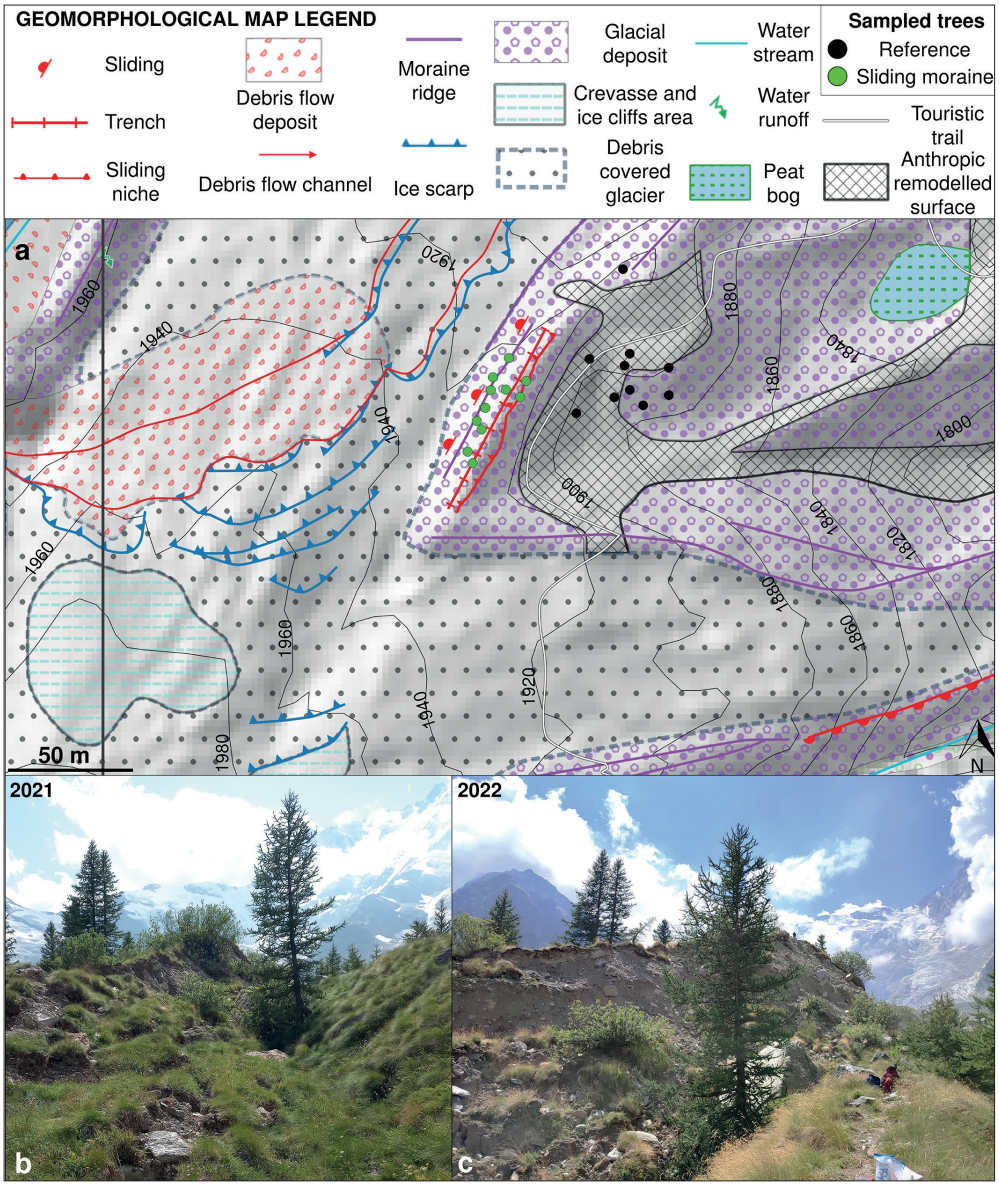

Fig. 4 Geomorphological map showing the location of the sampled trees on the right lateral moraine of the left lobe (a), and the trench in the timeframe 2021 (b) – 2022 (c).

4. Results and discussion

4.1 Geomorphological mapping and morphometric measurements

Fig. 4 (c) shows the geomorphological map with the sampled trees located in the area of the sliding moraine. The moraine ridge has moved towards the glacier debris-covered surface, favoring the opening of a trench. Moreover, the sliding niche is undergoing regressive erosion. The intensity of erosion is not homogeneous along the niche (Fig. 3). Tab. 2 shows the values measured for the time interval between 2018 and 2023 with the error estimated according to the orthophoto resolution. The considered timeframe begins one year before the fracture opening during the field survey in 2019 (2018, available orthophoto) reported in the literature (Mortara et al. 2023).

The average displacement rates related to the sliding of the moraine are comparable, within the error related to orthophoto resolution, both using the trail displacement (1.98 m/y, since 2018, or 2.47 m/y, since 2019; Tab. 2) and the tree canopies growing along the sliding moraine ridge (1.87 m/y, since 2018, or 2.34 m/y; Tab. 2). The average values for the time interval between 2021 and 2023 (1.78 m/y for the trail; 1.96 m/y for the moraine ridge; Tab. 1) are also comparable, within the error related to orthophoto resolution, with the sliding niche retreat rate in the same period (1.70 m/y; Tab. 1). During the analyzed time interval comparing the available orthophotos (2018–2023) the rates are quite constant. However, if we consider the year in which ground fracturing was surveyed on the field (i.e. 2019) for the rate calculation, a slowing-down of the sliding from the period between 2019 and 2021 (3.17 m/y for the trail; 2.72 m/y for

Tab. 2 Values of displacement and the related rates affecting the moraine sliding area. The (*) rates are calculated considering the year of displacement (2019) in relation to ground evidence (Mortara et al. 2023).

Process	Indicator	2018–2021 (m) (± 0.3 m)	2021–2023 (m) (± 0.3 m)	2018–2023 (m) (± 0.3 m)
Sliding	Trail displacement	2.96	4.27	7.22
		5.18	1.66	6.84
		8.68	4.17	12.85
		7.36	3.44	10.79
		7.52	4.22	11.74
	Average	**6.34**	**3.55**	**9.89**
	Rate	**2.11 (3.17*)**	**1.78**	**1.98 (2.47*)**
	Moraine ridge displacement	5.24	5.3	10.54
		5.60	5.32	10.92
		5.88	3.92	9.8
		5.17	4.35	9.52
		5.96	2.52	8.47
		6.48	2.11	8.58
		3.70	3.92	7.62
	Average	**5.43**	**3.92**	**9.35**
	Rate	**1.81 (2.72*)**	**1.96**	**1.87 (2.34*)**
Regressive erosion	Sliding niche displacement		5.41	
			5.25	
			2.55	
			3.46	
			3.5	
			2.75	
			7.92	
			2.97	
			3.83	
			1.04	
			4.03	
			2.26	
			1.05	
			1.51	
	Average		**3.40**	
	Rate		**1.70**	

the moraine ridge) to the period between 2021 and 2023 (1.78 m/y for the trail; 1.96 m/y for the moraine ridge) may be hypothesized. These data are discussed in relation to the tree and, especially, root information.

4.2 Dendrogeomorphological analyses

Tree cores

Fig. 5 shows the hillshade built from the 2023 DSM (Digital Surface Model), which highlights the presence of the trench. In the background, the minimum age of sampled trees is plotted. The oldest trees were present at least from the middle of the 1970s. These data agree with the orthophotos reconstruction (Fig. 6) where the trees were absent in 1951 and began to appear in 1989, when three trees had already germinated (Nos. 1, 5, and 6). In the 1990s, seven additional trees were present at least (Nos. 2, 14–19), while other nine tree ages indicated their presence from the 2000s (Nos. 3, 4, 7–9, 10, 12, and 13). The youngest are trees No. 8 and 11, less than 20 years old. The distribution of age is hence quite random in the moraine area, despite the fact that oldest trees (Nos. 1, 5, and 6) are located along the current erosion scarp.

Supplementary File A includes the evolution of the area through orthophotos since 1951, with the current position of trees plotted, and specific symbols to show their germination through time (i.e., minimum age).

The analysis of tree ring width anomalies (NAI) and of the CW in tree cores is summarized in Fig. 6, where the percentage of trees affected by NAI (for reference chronology and sliding moraine trees) and compression wood (only for the sliding moraine) are depicted, also indicating the number of trees growing in each year on the moraine area. The figure shows the timing of the most important glacial events interfering with the moraine, i.e., the surge-type event (the wider timeframe in which evidence is indicated in the literature; 1999–2003; Kääb et al. 2004) and the sliding (considering the field evidence from 2019; Mortara et al. 2023). In the first case, the moraine trees show a more intense NAI compared to the reference chronology, not so much during the event itself, but immediately after, in the years between 2003 and 2004 (30% of the trees with NAI < −40%). Even if two years of disturbance may be few to be considered a reliable response to a disturbing event, potentially this anomaly may be put in relation to the ground destabilization following the glacier downwasting. Indeed, the surge may have potentially affected the trees both during the event by the push provoked by the glacier overwhelming the moraine, or after the event, under debuttressing conditions. The reference chronology, on the other side, shows a more intense NAI only in 2004 (approximately 55% of the trees with NAI < −40%). Anyway, the less intense NAI in 2004 in the sliding moraine trees may be related to the NAI calculation itself, which considered the average of the previous four years. Since the NAI began in 2003, the disturbance may have been smoothed.

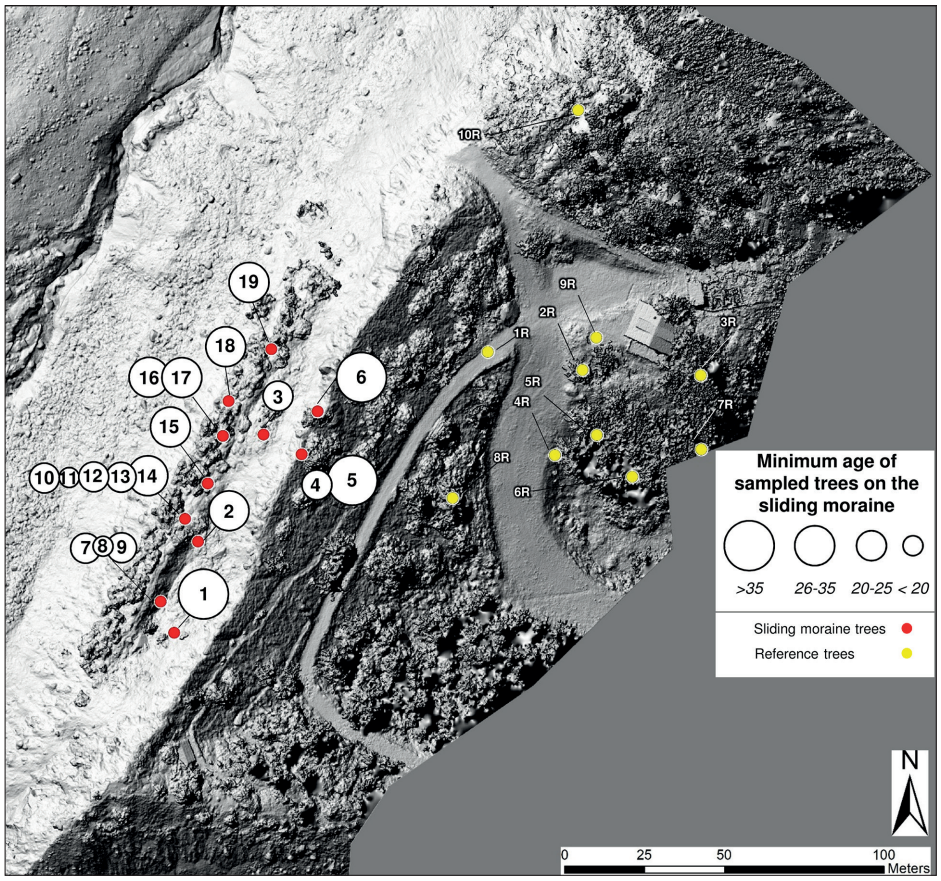

Fig. 5 Distribution of the minimum ages of sampled trees plotted on the 2023 Hillshade – Digital Surface Model from the UAV flight performed in August 2023 (resolution 0.05 m) (Brodský et al. 2024, in this issue), showing the trench in the sliding moraine.

Considering the meteorological conditions 2004 was not an extreme year neither in terms of temperature, nor drought conditions, hence they could not be considered as a potential influencer on tree ring growth. Later on, at the beginning of the sliding in 2019, the NAI does not prove to be a discriminant indicator between the reference chronology and sliding trees.

Concerning CW, the temporal distribution in relation to the number of trees is reported in Figure 6, and the spatio-temporal distribution of the compression wood for the timeframe 1997–2022 is presented in Supplementary File B. Compression wood is clearly present in the moraine tree rings since 2001, slightly after the beginning of the surge-type event. The increase during and after the surge is evident, and in some years particularly intensifying, probably due to the general relaxation of the inner flank of the moraine parallel to the glacier downwasting. Other information retrieved is the absence of specific spatial sub-clusters of trees featured by CW at different moments or with different intensities. Considering the sliding period from 2018 to 2019, different behavior may be expected between the trees on the niche, above the erosion scarp, and those located on the landslide body, as detected in other cases (e.g., Bollati et al. 2016). In this case, no significant distinction occurs, as the disturbance is distributed in the area quite homogeneously. Concerning climate and its direct relation with the sliding, and hence its indirect relation with tree growth, heavy and/or prolonged rains, as well as snow melting during very snowy years, may trigger sliding and water-runoff (Manconi and Giordan 2015). The CW peak recorded in 2009 may be related to the greater quantity of snow available until the late spring of 2009 and the intense related snow melting, destabilizing the moraine. The moraine flank relaxation finally evolved in 2019 in the form of ground fracturing and sliding (Mortara et al. 2023). In 2018, in particular, a slight peak is visible one year before the ground fracturing (Fig. 7; Supplementary File B). It is worth considering that some of the trees have maintained a relatively stable position, moving together with the moraine. This may have caused the apparent decrease in CW during the last period, with the trees being in a new and relative stable position during the sliding. As a final observation, no significant occurrences of TRDs were found in the tree cores, indicating that during the surge period, the glacier probably did not mechanically impact the trees on this moraine as occurred on other moraines (Mortara and Tamburini 2009).

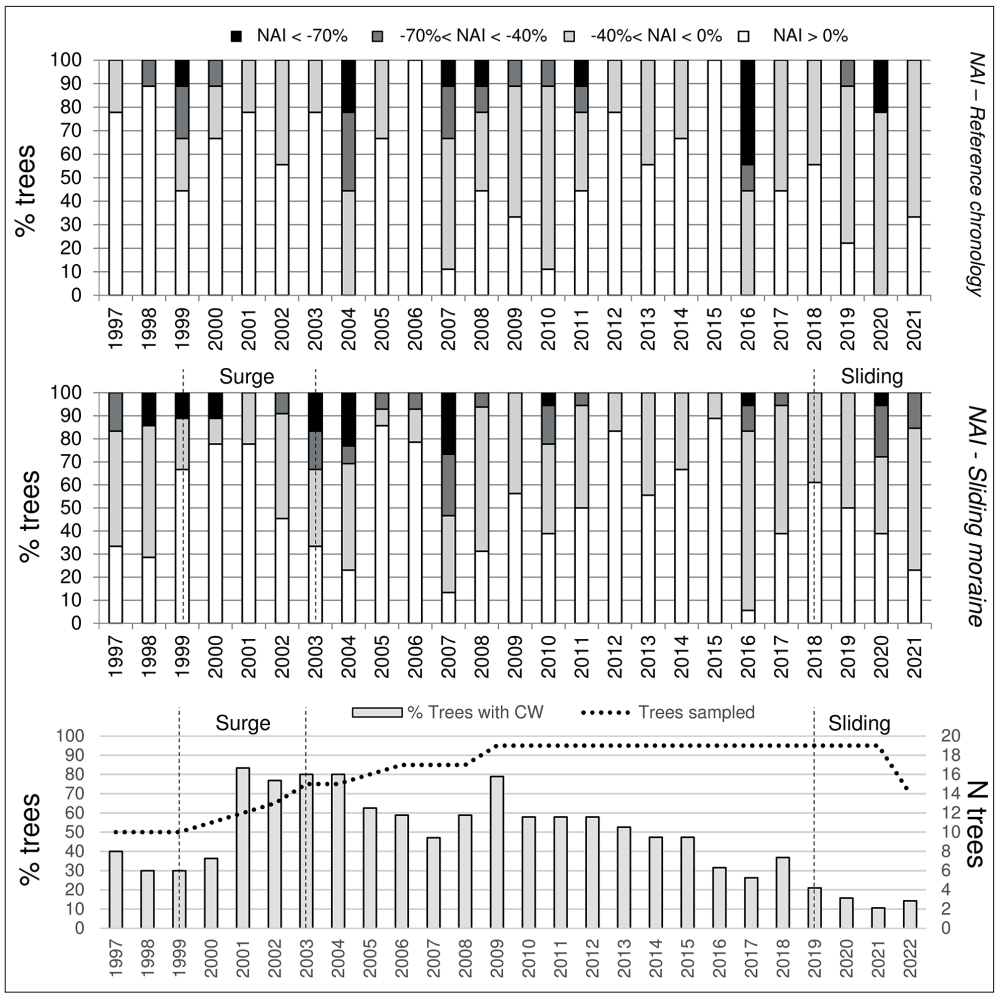

Fig. 6 Negative anomaly index (NAI) for the reference (first graph) and sliding (second graph) tree chronologies, and compression wood for sliding trees (third graph). The data are plotted since 1997, when at least 50% of the trees were present.

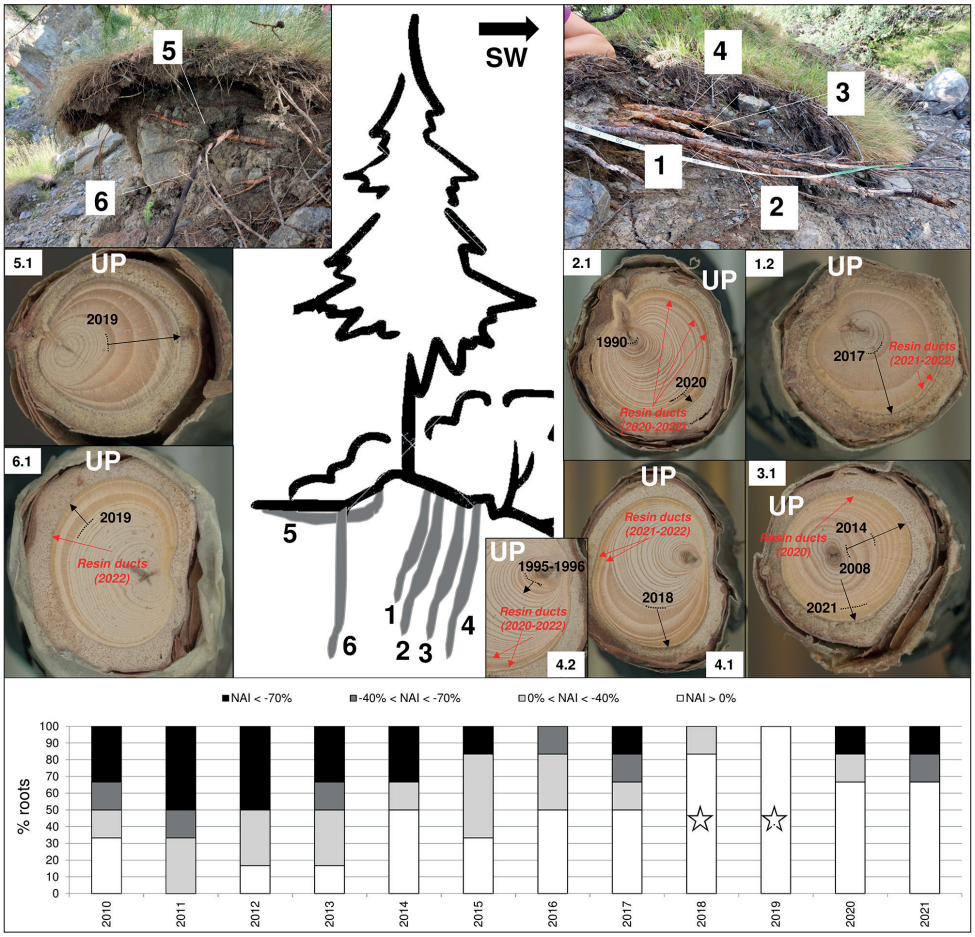

Fig. 7 Tree No. 6 and its sampled roots (1 to 6). Disks from some of the root samples indicating the main features (exposure year, traumatic resin ducts) as identified under the microscope. The graph below plots the NAI resulting for the timeframe between 2010 and 2021 with the white stars indicating the growth release in relation to the moraine sliding.

Root exposure

Along the detachment niche, despite some trees still being located in precarious positions, only one tree (No. 6 in fig. 5) showed roots suitable for sampling.

The main aim of the analysis was to detect the exposure year. Fig. 7 shows the root sections together with their position in the sampling field of tree No. 6.

The roots are concordant in showing an abrupt release in ring width in these last seven years, also testified by the NAI (white stars). Despite the field evidence of trenching along the moraine in 2019, one root shows an abrupt release in 2017 (root No. 1.2, Fig. 7), with the majority of roots showing an evident growth release in the period between 2018 and 2019 (e.g., Nos. 1 and 4), with a total positive growth anomaly (100% of the roots) in 2019, continuing, even if less intensely, to-date. This may be put in relation also with the peak of compression wood in the trunk cores in 2018 (Fig. 6). In two cases (root Nos. 2, and 4), a small peak in the 1990s was also identified, and in one of them (root No. 2) also in the second half of the 2000s, with an evident peak in 2009. As mentioned before 2009 was a year with an intense snow melting, potentially favoring local superficial denudation. Finally, very clear TRDs in the period between 2020 and 2021 in almost all the roots testify to disturbance.

4.3 Integration of geomorphic feature survey, morphometric measurements, and dendrogeomorphological data

According to De Gaetani et al. (2021), the period when the downwasting occurred in the glacier snout area, including the investigated moraine, is between 2009 and 2019. Nevertheless, the trees (trunk and roots) indicate instability conditions that, even if with different degree of intensity and spatio-temporal distribution, are uninterrupted since the surge-type event (2000–2002) to-date. Considering the dendrogeomorphological data of the roots and trunk cores, and the year 2018 as the first year with dendrogeomorphological signs of ground destabilization along the moraine, the average displacement rates of the trail calculated through morphometric techniques for the time interval between 2018 and 2023 seem to be the most realistic: 1.87–1.98 m/y (Tab. 2).

This would exclude the hypothesized slow-down of rates beginning in 2019 and previously discussed in Section 4.1. In this case, the temporal trend using 2018 for the trail (2.11 m/y to 1.78 m/y; Tab. 2), and for the moraine ridge (1.81 m/y to 1.96 m/y; Tab. 2) is discordant. Unfortunately, due to the continuous vegetation coverage and the unfavorable shadows, the orthophoto from 2018 could not be used to confirm these data.

The results from the tree analyses, field surveys, and morphometric measurements, if combined, may provide a more reliable time constraint, and consequently, movement rates to geomorphic processes. The limitation of remote sensing may be the time interval between the release of orthophoto or satellite images and their resolution, the presence of vegetation coverage or illumination and shadows, masking the geomorphic evidence (e.g., ground fracturing), while trees provide a yearly/seasonal time resolution. The remote sensing limitation, has recently been solved by the widespread use of UAV technology, allowing for very high-resolution acquisitions on demand within very short time intervals according to the type of events affecting an area, with the most adequate light conditions. The limitation of field surveys may be related to underground conditions that may not always produce sudden morphological effects at the topographic surface, but they may do earlier on trees and root systems. In this case, trees may reveal something already occurring below the surface (the roots are in the ground), while surface effects are not yet visible. However, in this specific case, the limit of dendrogeomorphology rely in the not-always clear signal in terms of NAI and CW, and, mainly, in the number of trees available for coring (trunks and roots). Concerning roots, specifically, since the data come in this case from only one tree specimen, the data obtained through the root exposure, even if very useful at punctual scale, could not be considered representative of the erosive regression along the whole detachment niche, as testified by the different values obtained along it from the morphometric measurements (Tab. 2).

5. Concluding remarks

Since a portion of the Belvedere Glacier is located below the tree line, it serves as a compelling study case for investigating glacier dynamics through a multidisciplinary approach, including morphometry, geomorphological survey and mapping, and dendrogeomorphological analyses. Besides the debris coverage providing a form of ecologic support role towards organisms, as highlighted in the literature, the glacial dynamic affects the vegetation growing on glacial depositional landforms such as the lateral moraine. This study has enabled the detection of signals in tree rings (growth anomalies, compression wood) and root rings (growth release and traumatic resin ducts), even if it was not always easy to disentangle. Nevertheless, information about the timing of glacial and geomorphological events affecting the right moraine of the left lobe of the glacier has been retrieved and discussed. The oldest trees were present at least from the middle of the1970s, and, considering the surge-type event, they record the peak of disturbance in terms of NAI in the period between 2003 and 2004, slightly after the acme of the surge-type event. Compression wood indicates disturbance since 2001, slightly after the beginning of the surge-type event, and prosecuting also in the following years, even if diminishing. The trench opening in the ground, surveyed in the literature in 2019, is preceded by a slight peak in compression wood already present in 2018. These data are also confirmed by the roots that show in one case an abrupt release in 2017, with the majority of growth release in the period between 2018 and 2019, continuing, even if less intensely, to-date. Moreover, roots show in these last years a disturbance in the form of very evident TRDs. Finally, the average displacement rates along the moraine calculated for the time interval between 2018 and 2023 are 1.87–1.98 m/y, while the regression rate of the sliding niche was also calculated to be 1.70 m/y (2021–2023).

To conclude, considering the limits of all the techniques applied, the integration of different techniques and a multidisciplinary approach are essential for delineating the dynamic features of a complex geomorphological and glaciological context like the Belvedere Glacier environment. Discussing these dynamics is relevant not only for the glacier site but it may provide information for managing hazard scenarios also affecting downvalley areas.

Acknowledgements

The project was funded in the aim of the 4EU+ European University Alliance, with the Mini grants afforded to Charles University in Prague (*Multidisciplinary approaches to assess the evolution of glacial and periglacial areas in the Alps under climate change conditions; Remote Sensing of the Cryosphere Dynamics under the Influence of Climate Change: a 4EU+ Project to investigate the evolving glacial environment*), grant number 4EU+/23/F4/19. The work was also partly supported by the Italian Ministry for Universities and Research (MUR) through the projects "Dipartimenti di Eccellenza 2018–22" (*Le Geoscienze per la società: risorse e loro evoluzione*) and "Dipartimenti di Eccellenza 2023–27" and (*Le Georisorse per la transizione ecologica e lo sviluppo territoriale*) and through the PRIN (Progetto di Ricerca di Rilevante Interesse Nazionale) (GEOTRes – Geoheritage threating and resilience: mapping the impact of geomorphic and human processes in sensitive morphoclimatic environments); by University of Milan through the Sostegno alla ricerca Project 2021(*Indicatori geomorfologici e geopedologici per ricostruire l'evoluzione delle aree di recente deglaciazione;* grant number PSR2021 _RAZZONI) and 2022 (*Evoluzione dei processi geomorfologici e degli impatti sul ciclo idrologico in contesti sensibili al cambiamento climatico;* grant number PSR2022_RAZZONI). The Authors would like to thank the Province of Verbano-Cusio-Ossola for the permit of UAV and dendrogeomorphological surveys

(dr. Andrea De Zordi, Settore III – Assetto del Territorio Georisorse e Tutela Faunistica, Servizio Rete Natura 2000 e Forestazione).

References

Azzoni, R. S., Franzetti, A., Fontaneto, D., Zullini, A., Ambrosini, R. (2015): Nematodes and rotifers on two Alpine debris-covered glaciers. Italian Journal of Zoology 82(4), 616–623, https://doi.org/10.1080/11250003.2015.1080312.

Azzoni, R. S., Pelfini, M., Zerboni, A. (2023): Estimating the evolution of a Post-Little Ice Age deglaciated Alpine Valley through the DEM of Difference (DoD). Remote Sensing 15(12), 3190, https://doi.org/10.3390/rs15123190.

Ballantyne, C. K. (2002): Paraglacial geomorphology. Quaternary Science Reviews 21(18–19), 1935–2017, https://doi.org/10.1016/S0277-3791(02)00005-7.

Benn, D. I., Bolch, T., Hands, K., Gulley, J., Luckman, A., Nicholson, L. I., Quincey D., Thompson T., Toumi R., Wiseman, S. (2012): Response of debris-covered glaciers in the Mount Everest region to recent warming, and implications for outburst flood hazards. Earth-Science Reviews 114(1–2), 156–174, https://doi.org/10.1016/j.earscirev.2012.03.008.

Bodoque, J. M., Ballesteros-Cánovas, J. A., Lucía, A., Díez-Herrero, A., Martín-Duque, J. F. (2015): Source of error and uncertainty in sheet erosion rates estimated from dendrogeomorphology. Earth Surface Processes and Landforms 40, 1146–1157, https://doi.org/10.1002/esp.3701.

Bodoque, J. M., Ballesteros-Cánovas, J. A., Lucía, A., Díez-Herrero, A., Martín-Duque, J. F. (2015): Source of error and uncertainty in sheet erosion rates estimated from dendrogeomorphology. Earth Surface Processes and Landforms 40(9), 1146–1157, https://doi.org/10.1002/esp.3701.

Bollati, I., Leonelli, G., Vezzola, L., Pelfini, M. (2015): The role of Ecological Value in Geomorphosite assessment for the Debris-Covered Miage Glacier (Western Italian Alps) based on a review of 2.5 centuries of scientific study. Geoheritage 7, 119–135, https://doi.org/10.1007/s12371-014-0111-2.

Bollati, I. M., Pellegrini, M., Reynard, E., Pelfini, M. (2017): Water driven processes and landforms evolution rates in mountain geomorphosites: examples from Swiss Alps. Catena 158, 321–339, https://doi.org/10.1016/j.catena.2017.07.013.

Bollati, I. M., Crosa Lenz, B., Golzio, A., Masseroli, A. (2018): Tree rings as ecological indicator of geomorphic activity in geoheritage studies. Ecological indicators 93, 899–916, https://doi.org/10.1016/j.ecolind.2018.05.053.

Bollati, I. M., Masseroli, A., Mortara, G., Pelfini, M., Trombino, L. (2019): Alpine gullies system evolution: erosion drivers and control factors. Two examples from the western Italian Alps. Geomorphology 327, 248–263, https://doi.org/10.1016/j.geomorph.2018.10.025.

Bollati, I. M., Viani, C., Masseroli, A., Mortara, G., Testa, B., Tronti, G., Pelfini M., Reynard, E. (2023): Geodiversity of proglacial areas and implications for geosystem services: A review. Geomorphology 421, 108517, https://doi.org/10.1016/j.geomorph.2022.108517.

Bollati, I. M., Cavalli, M., Masseroli, A., Viani, C., Moraschina, F., Pelfini, M. (2024): Thematic mapping for sediment cascade analysis in small mountain catchments – The case of the Buscagna valley (Lepontine Alps). Geomorphology 446, 109001, https://doi.org/10.1016/j.geomorph.2023.109001.

Bollschweiler, M., Stoffel, M., Schneuwly, D. M., Bourqui, K. (2008): Traumatic resin ducts in Larix decidua stems impacted by debris flows. Tree physiology 28(2), 255–263, https://doi.org/10.1093/treephys/28.2.255.

Caccianiga, M., Andreis, C., Diolaiuti, G., D'Agata, C., Mihalcea, C., Smiraglia, C. (2011): Alpine debris-covered glaciers as a habitat for plant life. The Holocene 21(6), 1011–1020, https://doi.org/10.1177/0959683611400219.

Chiarle, M., Iannotti, S., Mortara, G., Deline, P. (2007): Recent debris flow occurrences associated with glaciers in the Alps. Global and Planetary Change 56(1–2), 123–136, https://doi.org/10.1016/j.gloplacha.2006.07.003.

Church, M., Ryder, J. M. (1972): Paraglacial sedimentation: a consideration of fluvial processes conditioned by glaciation. Geological Society of America Bulletin 83(10), 3059–3072, https://doi.org/10.1130/0016-7606(1972)83[3059:PSACOF]2.0.CO;2.

Cook, E. R. (1985): A time series approach to tree-ring standardization. PhD thesis, University of Arizona.

Cruickshank, M. G., Lejour, D., Morrison, D. J. (2006): Traumatic resin canals as markers of infection events in Douglas-fir roots infected with Armillaria root disease. Forest Pathology 36(5), 372–384, https://doi.org/10.1111/j.1439-0329.2006.00469.x.

Curry, A. M., Ballantyne, C. K. (1999): Paraglacial modification of glacigenic sediment. Geografiska Annaler, Series A: Physical Geography 81(3), 409–419, https://doi.org/10.1111/j. 0435-3676.1999.00070.x.

De Bouchard d'Aubeterre, G., Favillier, A., Mainieri, R., Saez, J. L., Eckert, N., Saulnier, M., Peiry, J. L., Stoffel, M., Corona, C. (2019): Tree-ring reconstruction of snow avalanche activity: Does avalanche path selection matter? Science of the Total Environment 684, 496–508, https://doi.org/10.1016/j.scitotenv.2019.05.194.

De Gaetani, C. I., Ioli, F., Pinto, L. (2021): Aerial and UAV Images for Photogrammetric Analysis of Belvedere Glacier Evolution in the Period 1977–2019. Remote Sensing 13(18), 3787, https://doi.org/10.3390/rs13183787.

Diolaiuti, G., D'Agata, C., Smiraglia, C. (2003): Belvedere Glacier, Monte Rosa, Italian Alps: Tongue Thickness and Volume Variations in the Second Half of the 20th Century. Arctic Antarctic Alpine Research 35, 255–263, https://doi.org/10.1657/1523-0430(2003)035[0255:BGMRIA]2.0.CO;2.

Eckstein, D., Bauch, J. (1986): Beitrag zur Rationalisierung eines dendrochronologischen Verfahrens und zur Analyse seiner Aussagesicherheit. Forstwiss. Centralblatt 88, 230–250, https://doi.org/10.1007/BF02741777.

Fantucci, R. (1997): La dendrogeomorfologia nello studio della dinamica dei versanti: alcune recenti applicazioni in Italia. Geologia tecnica e ambientale 2/97, 21– 31.

Favillier, A., Guillet, S., Lopez-Saez, J., Giacona, F., Eckert, N., Zenhäusern, G., Peiry, J. L., Stoffel, M., Corona, C. (2023): Identifying and interpreting regional signals in tree-ring based reconstructions of snow avalanche activity in the Goms valley (Swiss Alps). Quaternary Science Reviews

307: 108063, https://doi.org/10.1016/j.quascirev.2023.108063.

Fyffe, C. L., Reid, T. D., Brock, B. W., Kirkbride, M. P., Diolaiuti, G., Smiraglia, C., Diotri, F. (2014): A distributed energy-balance melt model of an alpine debris-covered glacier. Journal of Glaciology 60(221), 587–602, https://doi.org/10.3189/2014JoG13J148.

Garavaglia, V., Pelfini, M., Bini, A., Arzuffi, L., Bozzoni, M. (2009): Recent evolution of debris-flow fans in the Central Swiss Alps and associated risk assessment: two examples in Roseg Valley. Physical Geography 30(2), 105–129, https://doi.org/10.2747/0272-3646.30.2.105.

Garavaglia, V., Pelfini, M., Motta, E. (2010): Glacier stream activity in the proglacial area of an italian debris-covered glacier: an application of dendroglaciology. Geografia Fisica e Dinamica Quaternaria 33(1), 2010, 15–24.

Garavaglia, V., Pelfini, M. (2011): The role of border areas for dendrochronological investigations on catastrophic snow avalanches: a case study from the Italian Alps. Catena 87(2), 209–215, https://doi.org/10.1016/j.catena.2011.06.006.

Giordan, D., Lanteri, L., Fioraso, G., Bormioli, D., Luino, F., Turconi, L., Chiarle, M., Mortara, G., Tamburini, A. (2022): Itinerario 2.3. Frane in alta quota: il Ghiacciaio del Belvedere e la parete Est del Monte Rosa. In: Calcaterra, D., Cencetti, C., Meisina, C., Revellino, P., Frane d'Italia. Associazione Italiana Geologia Applicata Ambientale. Luciano Ed., pp. 81–84.

Gray, M., Gordon, J. E., Brown, E. J. (2013): Geodiversity and the ecosystem approach: the contribution of geoscience in delivering integrated environmental management. Proceedings of the Geologists' Association 124(4), 659–673, https://doi.org/10.1016/j.pgeola.2013.01.003.

Guida, D., Pelfini, M., Santilli, M. (2008): Geomorphological and dendrochronological analyses of a complex landslide in the Southern Apennines. Geografiska Annaler: Series A, Physical Geography 90(3), 211–226, https://doi.org/10.1111/j.1468-0459.2008.340.x.

Haeberli, W., Kääb, A., Paul, F., Chiarle, M., Mortara, G., Mazza, A., Deline P., Richardson, S. (2002). A surge-type movement at Ghiacciaio del Belvedere and a developing slope instability in the east face of Monte Rosa, Macugnaga, Italian Alps. Norsk Geografisk Tidsskrift – Norwegian Journal of Geography 56(2), 104–111, https://doi.org/10.1080/002919502760056422.

Hupp, C., Carey, W. P. (1990): Dendrogeomorphic approach to estimating slope retreat. Geology 18, 658–661, https://doi.org/10.1130/0091-7613(1990)018%3C0658:DATESR%3E2.3.CO;2.

Ioli, F., Bianchi, A., Cina, A., De Michele, C., Maschio, P., Passoni, D., Pinto, L. (2021): Mid-term monitoring of glacier's variations with UAVs: The example of the Belvedere Glacier. Remote Sensing 14(1), 28, https://doi.org/10.3390/rs14010028.

Ioli, F., Bruno, E., Calzolari, D., Galbiati, M., Mannocchi, A., Manzoni, P., Martini, M., Bianchi, A., Cina, A., De Michele, C., Pinto, L. (2023): A replicable open-source multi-camera system for low-cost 4D glacier monitoring. International Archives of the Photogrammetry, Remote Sensing and Spatial Information Sciences (ISPRS Archives), XLVIII-M-1-2023, 137–144, https://doi.org/10.5194/isprs-archives-XLVIII-M-1-2023-137-2023.

Ivy-Ochs, S., Kerschner, H., Maisch, M., Christl, M., Kubik, P. W., Schlüchter, C. (2009): Latest Pleistocene and Holocene glacier variations in the European Alps. Quaternary Science Reviews 28(21–22), 2137–2149, https://doi.org/10.1016/j.quascirev.2009.03.009.

Kääb, A., Huggel, C., Barbero, S., Chiarle, M., Cordola, M., Epifani, F., Haebelri, W., Mortara, G., Semino, P., tamburini, A., Viazzo, G. (2004) Glacier hazards at Belvedere Glacier and the Monte Rosa East Face, Italian Alps: processes and mitigation. INTERPRAEVENT 2004–RIVA/TRIENT., pp. 67–78.

Kääb, A., Huggel, C., Fischer, L., Guex, S., Paul, F., Roer, I., Salzmann, N., Schlaefli, S., Schmutz, K., Schneider, D., Strozzi, T., Weidmann, Y. (2005): Remote sensing of glacier-and permafrost-related hazards in high mountains: An overview. Natural Hazard Earth Systems 5, 527–554, https://doi.org/10.5194/nhess-5-527-2005.

Klimeš, J., Novotný, J., Novotná, I., Jordán de Urries, B., Vilímek, V., Emmer, A., Strozzi, T., Kusák, M., Rapre, A. C., Hartvich, F., Frey, H. (2016): Landslides in moraines as triggers of glacial lake outburst floods: example from Palcacocha Lake (Cordillera Blanca, Peru). Landslides 13(6), 1461–1477, https://doi.org/10.1007/s10346-016-0724-4.

Leonelli, G., Pelfini, M., Cherubini, P. (2008): Exploring the potential of tree-ring chronologies from the Trafoi Valley (Central Italian Alps) to reconstruct glacier mass balance. Boreas 37, 169–198, https://doi.org/10.1111/j.1502-3885.2007.00010.x.

Leonelli, G., Pelfini, M. (2013): Past surface instability of Miage debris-covered glacier tongue (Mont Blanc Massif, Italy): a decadal-scale tree-ring-based reconstruction. Boreas 42, 613–622, https://doi.org/10.1111/j.1502-3885.2012.00291.x.

Leonelli, G., Coppola, A., Baroni, C., Salvatore, M. C., Maugeri, M., Brunetti, M., Pelfini, M. (2016): Multispecies dendroclimatic reconstructions of summer temperature in the European Alps enhanced by trees highly sensitive to temperature. Climatic Change 137, 275–291, https://doi.org/10.1007/s10584-016-1658-5.

Manconi, A., Giordan, D. (2015): Landslide early warning based on failure forecast models: the example of the Mt. de La Saxe rockslide, northern Italy, Natural Hazards and Earth System Science 15(7), 1639–1644, https://doi.org/10.5194/nhess-15-1639-2015.

Mazza, A. (1998): Evolution and dynamics of Ghiacciaio Nord delle Locce (Valle Anzasca, Western Alps) from 1854 to the present. Geografia Fïsica e Dinamica Quaternaria 21, 233–243.

Mazza, A. (2003): The kinematics wave theory: a possible application to "Ghiacciaio del Belvedere" (Valle Anzasca, Italian Alps). Preliminary hypothesis. Terra glacialis 6, 23–36.

Mehta, M., Kumar, V., Kunmar, P., Sain, K. (2023): Response of the Thick and Thin Debris-Covered Glaciers between 1971 and 2019 in Ladakh Himalaya, India – A Case Study from Pensilungpa and Durung-Drung Glaciers. Sustainability 15(5): 4267, https://doi.org/10.3390/su15054267.

Monterin, U. (1923): Il Ghiacciaio di Macugnaga dal 1870 al 1922. Bollettino del Comitato Glaciologico Italiano 5, 12–40.

Mortara, G., Chiarle, M., Tamburini, A., Mercalli, L., Cat Berro, D. (2023): a vent'anni dal Lago Effimero (Ghiacciaio del Belvedere, Monte Rosa): eredità di un evento emblematico per le Alpi. Nimbus 90, 26–41.

Mortara, G., Carton, A., Chiarle, M., Tamburini, A. (2017). Ai piedi della parete più alta delle Alpi. In: Società Geologica Italiana, Itinerari glaciologici nella Alpi Italiane – Il ghiacciaio del Belvedere al Monte Rosa. Guide Geologiche Regionali 12 193–214.

Mourey, J., Ravanel, L., Lambiel, C. (2022): Climate change related processes affecting mountaineering itineraries, mapping and application to the Valais Alps (Switzerland). Geografiska Annaler: Series A, Physical Geography 104(2), 109–126, https://doi.org/10.1080/04353676.2022.2064651.

Nakawo, M., Yabuki, H., Sakai, A. (1999): Characteristics of Khumbu Glacier, Nepal Himalaya: recent change in the debris-covered area. Annals of Glaciology 28, 118–122, https://doi.org/10.3189/172756499781821788.

Paleari, M. (2014) Evoluzione delle pareti alpine di alta montagna ed effetti sull'approccio alpinistico: l'esempio dell'alta Valle Anzasca, Parete Est del Monte Rosa, Italia. Unpublished thesis.

Paul, F., Rastner, P., Azzoni, R. S., Diolaiuti, G., Fugazza, D., Le Bris, R., Nemec, J., Rabatel, A., Ramusovic, M., Schwaizer, G., Smiraglia, C. (2020): Glacier shrinkage in the Alps continues unabated as revealed by a new glacier inventory from Sentinel-2. Earth System Science Data 12(3), 1805–1821, https://doi.org/10.5194/essd-12-1805-2020.

Pelfini, M. (1999): Dendrogeomorphological study of glacier fluctuations in the Italian Alps during the Little Ice Age. Annals of Glaciology 28, 123–128, https://doi.org/10.3189/172756499781821634.

Pelfini, M., Santilli, M. (2006): Dendrogeomorphological analyses on exposed roots along two mountain hiking trails in the Central Italian Alps. Geografiska Annaler, Series A: Physical Geography 88(3), 223–236, https://doi.org/10.1111/j.1468-0459.2006.00297.x.

Pelfini, M., Santilli, M., Leonelli, G., Bozzoni, M. (2007): Investigating surface movements of debris-covered Miage glacier, Western Italian Alps, using dendroglaciological analysis. Journal of Glaciology 53(180), 141–152, https://doi.org/10.3189/172756507781833839.

Pelfini, M., Diolaiuti, G., Leonelli, G., Bozzoni, M., Bressan, N., Briosch, D., Riccardi, A. (2012): The influence of glacier surface processes on the short-term evolution of supraglacial tree vegetation: The case study of the Miage Glacier, Italian Alps. The Holocene 22(8), 847–857, https://doi.org/10.1177/0959683611434222.

Richter, M., Fickert, T., Gruninger, F. (2004): Pflanzen auf schuttbedeckten Gletschern – wandernde Kuriositaten. Geooko [Bensheim] 25(3/4), 225–256.

Schmidt, B. (1987): Ein dendrochronologischer Befund zum Bau der Stadtmauer der Colonia Ulpia Traiana. Bonner Jahrbuch 187.

Serandrei-Barbero, R., Donnici, S., Zecchetto, S. (2022). Past and future behavior of the valley glaciers in the Italian Alps. Frontiers in Earth Science 10, 972601, https://doi.org/10.3389/feart.2022.972601.

Smiraglia, C., Diolaiuti, G. A. (2015): The New Italian Glacier Inventory; Ev-K2-CNR: Bergamo, Italy. Available online https://sites.unimi.it/glaciol/index.php/en/italian-glacier-inventory (accessed on 20. 2. 2024).

Stoffel, M., Bollschweiler, M. (2008): Tree-ring analysis in natural hazards research–an overview. Natural Hazards and Earth System Sciences 8(2), 187–202, https://doi.org/10.5194/nhess-8-187-2008.

Stoffel, M., Corona, C., Ballesteros-Cánovas, J. A., Bodoque, J. M. (2013): Dating and quantification of erosion processes based on exposed roots. Earth-Science Reviews 123, 18–34, https://doi.org/10.1016/j.earscirev.2013.04.002.

Tamburini, A., Chiarle, M., Mortara, G. (2019): Il collasso delle morene del Ghiacciaio del Belvedere. www.nimbus.it/ghiacciai/2019/190816_BelvedereCollassoMorene.htm.

Tampucci, D., Azzoni, R. S., Boracchi, P., Citterio, C., Compostella, C., Diolaiuti, G., Isaia, M., Marano, G., Smiraglia, C., Gobbi, M., Caccianiga, M. (2017): Debris-covered glaciers as habitat for plant and arthropod species: Environmental framework and colonization patterns. Ecological Complexity 32(Part A), 42–52, https://doi.org/10.1016/j.ecocom.2017.09.004.

Tichavský, R., Kluzová, O., Šilhán, K. (2019): Differences between the responses of European larch (Larix decidua Mill.) and Norway spruce (Picea abies (L.) Karst) to landslide activity based on dendrogeomorphic and dendrometric data. Geomorphology 330, 57–68, https://doi.org/10.1016/j.geomorph.2019.01.013.

VAW (Versuchsanstalt for Wasserbau, Hydrologie und Glaziologi, ETH Zürich) (1983–1985): Ricerche glaciologiche al Lago delle Locce, Macugnaga, Italia; Studi sul comportamento del Ghiacciaio del Belvedere, Macugnaga, Italia; Valutazione dei rischi glaciali nella Regione Macugnaga/Monte Rosa, Relazioni Nr. 97.2, 97.3, 97.4 per La Comunitá Montana della Valle Anzasca.

Vejpustková, M., Holuša, J. (2006): Impact of defoliation caused by the sawfly Cephalcia lariciphila (Hymenoptera: Pamphilidae) on radial growth of larch (Larix decidua Mill.). European Journal of Forest Research 125, 391–396, https://doi.org/10.1007/s10342-006-0112-z.